Metallophysics and Advanced Technologies
Металофіз. новітні технол.
Metallofiz. Noveishie Tekhnol.
2023, vol. 45, No. 1, pp. 55–63
https://doi.org/10.15407/mfint.45.01.0055
Reprints available directly from the publisher

© 2023 Publishing House 'Akademperiodyka',
National Academy of Sciences of Ukraine
Published by license under
the G. V. Kurdyumov Institute for Metal Physics–
N.A.S. of Ukraine Publishers imprint.
Printed in Ukraine.

PACS numbers: 61.05.cp, 66.30.Lw, 68.35.Fx, 68.55.Ln, 81.15.Cd, 82.80.Ms

Effect of Layers' Inversion on Thermally Induced Diffusion in Thin Ni/Ti Films

A. K. Orlov, I. O. Kruhlov, I. E. Kotenko[*], and S. M. Voloshko

National Technical University of Ukraine
'Igor Sikorsky Kyiv Polytechnic Institute',
37 Peremohy Ave.,
UA-03056 Kyiv, Ukraine
[*]*L. V. Pisarzhevsky Institute of Physical Chemistry, N.A.S. of Ukraine,*
31 Nauky Ave.,
03028 Kyiv, Ukraine

In this study, bilayer thin films with different layers' order, Ni/Ti/Si (100) and Ti/Ni/Si (100), are prepared by magnetron sputtering at room temperature followed by the thermal annealing in a vacuum in the temperature range from 400°C to 600°C for 1 h. The combination of XRD and SIMS techniques is used to investigate the effect of the layers' inverse arrangement on the crystalline structure, phase formation and elemental composition upon thermal treatment. As revealed, the annealing of the Ni/Ti bilayer leads to the diffusion of Ti atoms through the Ni grain boundaries towards the outer surface. For the case of Ti/Ni bilayer, interdiffusion between Ni and Ti is not detected upon heat treatment, whereas the thermally induced diffusion between Ni and substrate resulted in the formation of NiSi silicides is revealed. The likely structural and thermodynamic reasons for such behaviour are discussed.

Key words: thin films, NiTi, diffusion, thermal annealing, solid-state reactions.

У даному дослідженні двошарові тонкі плівки з різним порядком шарів, — Ni/Ti/Si (100) і Ti/Ni/Si (100), — було одержано методою магнетронного осадження за кімнатної температури з подальшим термічним відпалом у вакуумі в температурному інтервалі від 400°C до 600°C упродовж 1 год. З метою дослідження впливу інверсії розташування шарів на кристалічну

Corresponding author: Andriy Kostyantynovych Orlov
E-mail: orlov@kpm.kpi.ua

Citation: A. K. Orlov, I. O. Kruhlov, I. E. Kotenko, and S. M. Voloshko, Effect of Layers' Inversion on Thermally Induced Diffusion in Thin Ni/Ti Films, *Metallofiz. Noveishie Tekhnol.*, **45**, No. 1: 55–63 (2023). DOI: 10.15407/mfint.45.01.0055

структуру, фазоутворення та хемічний склад після термічного оброблення застосовано комбінацію метод РСФА і ВІМС. Виявлено, що відпал двошарової системи Ni/Ti зумовлює дифузію атомів Ti через шар Ni за зерномежовим механізмом до зовнішньої поверхні. У випадку системи Ti/Ni дифузійна взаємодія між Ni і Ti під час термічного оброблення відсутня, тоді як термічно індукована дифузія між Ni і підкладинкою приводить до утворення силіцидів NiSi. Обговорюються ймовірні структурні та термодинамічні причини такої поведінки.

Ключові слова: тонкі плівки, NiTi, дифузія, термічний відпал, твердотільні реакції.

(Received October 4, 2022)

1. INTRODUCTION

NiTi is one of the most well-known representatives of shape memory alloys (SMA) which are widely applied in biomedicine [1]. However, the set of unique properties of NiTi alloys such as large recoverable strain, high work output and good corrosion resistance enables their high potential of application in micro- and nanoelectromechanical systems (MEMS and NEMS) as thin-film actuators and sensors [2]. Besides, the annealing of Ni–Ti thin-film system is one of the routes to form Ni silicides [3, 4], which are widely used in silicon integrated circuit devices due to their high electrical conductivity, temperature stability, and corrosion resistance [5].

To achieve the desired functional properties, NiTi thin films are conventionally fabricated by physical vapour deposition (*e.g.*, by magnetron sputtering) of equiatomic alloy from a high-purity NiTi target [6]. An alternative approach is the sequential deposition of Ni and Ti separated metal layers followed by their thermally induced diffusion intermixing and formation of intermetallic phases. One of the advantages of the alternately deposited Ni and Ti layers is connected with the appearing of the shape memory effect at a lower annealing temperature as compared with annealed NiTi alloy thin films [7], which are usually condensed in an amorphous state during PVD growth. Furthermore, the deposition of Ni/Ti layered stacks with separate metal layers promotes the formation of fine grain microstructure even being heated to high temperatures [8]. It also enables better control over the chemical composition and in-depth homogeneity [9] of the final product as compared with the conventional NiTi alloy deposition as well.

As worth noting, during the synthesis of the Ni/Ti layered thin films, the sequence of deposited layers could strongly affect the thermally induced structural phase transitions and consequently the functional properties of the system. Depending on the application scope, the order of Ni and Ti layers deposition could vary, while there is no

widely accepted regularity on the metals' arrangement. Sometimes, Ni is applied as a top layer material and Ti as a bottom layer [9–11], while, in other studies, the inverse layers configuration with Ti as a top and Ni as a bottom layer is successfully utilized [12–14]. However, for the authors' best knowledge, the effect of the Ni and Ti layer alteration on the diffusion-controlled reactions and structural phase formation has not been studied directly yet.

Therefore, this study is aimed to reveal the influence of the deposited layers sequence on the features of diffusion, phase formation and chemical elements depth distribution in the thin Ni/Ti/Sub. and Ti/Ni/Sub. films annealed in the temperature range from 400°C to 600°C in a vacuum (10^{-3} Pa).

2. METHODS AND OBJECT

Two series of bilayer thin films with inverse order of layers, namely Ni/Ti/Sub. and Ti/Ni/Sub. (which will be referred to as Ni/Ti and Ti/Ni, respectively, in the following text), were prepared by magnetron sputtering onto Si (100) substrate from high-purity targets at room temperature. The thickness of layers was adjusted to 100 nm and 400 nm and was controlled using the quartz microbalance. Before the deposition, substrates were subjected to standard RCA cleaning procedure. After the deposition, thin films were annealed in a vacuum of 10^{-3} Pa in the temperature range from 400°C to 600°C for 1 hour using a heating rate of about 2°C/s. The temperature upon annealing was measured using the K-type thermocouple mounted at the samples' surface.

For phase identification and structural characterization, XRD measurement was accomplished in θ–2θ scanning geometry on a Rigaku ULTIMA IV diffractometer equipped with 1.5405 Å (CuK_α) x-ray source. XRD patterns were recorded at room temperature under the similar conditions for all samples. An average crystallite size in thin films was estimated using Scherrer's equation [15] by determining the broadening of the diffraction lines using Gaussian approximation. It should be noted that the applied approach did not consider the microstrains in the crystal, which could also contribute to the diffraction peak broadening.

Chemical elements distribution was studied by secondary ion mass spectrometry (SIMS) technique at MC-7201M device. Primary beam of Ar^+ ions with 10 keV-energy was applied for the etching, while the discharge current of the gun was of 0.4 mA, current density was of 2 μA/mm^2, and the basic pressure in the chamber was of $5.5 \cdot 10^{-5}$ Pa. In addition to the primary components of the film, the distribution of C^{12} and O^{16} light impurities secondary ions through the stack depth was also obtained.

3. EXPERIMENTAL RESULTS

Figure 1, *a* shows the θ–2θ XRD scans of the Ni/Ti bilayer films after deposition and annealing in vacuum in the temperature range of 400–600°C for 1 h. For the as-deposited Ni/Ti, two peaks are clearly seen at 44.62° and 52.06° diffraction angles, corresponding to the **(111)** and **(200)** fundamental peaks of face-centred cubic (f.c.c.) Ni phase. The absence of diffraction peaks from Ti layer most likely indicates its amorphous structure as formed at the deposition stage, which has been already observed in other studies [16].

Annealing in vacuum at 400°C does not induce the change of the phase composition of the system, the diffraction pattern looks very similar to the one obtained from as-deposited film. The phase composition of the Ni/Ti film remains unchanged even after the higher temperatures of 500°C and 600°C were applied. The only difference between the diffraction scans is observed in the slight redistribution of integral intensity of the Ni **(111)** and **(200)** diffraction peaks fixed for

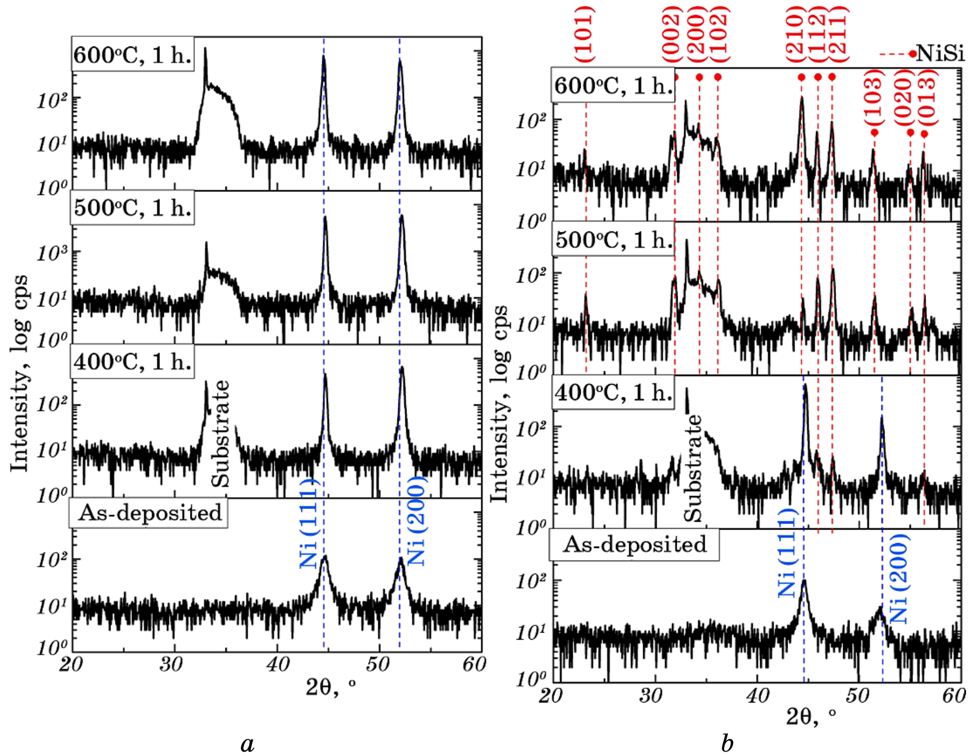

Fig. 1. XRD scans of thin Ni/Ti (*a*) and Ti/Ni (*b*) films after deposition and annealing in a vacuum at 400°C, 500°C and 600°C for 1 h.

the higher temperatures as compared to the 400°C annealing.

The as-deposited Ti/Ni film demonstrates the similar diffraction spectrum to the one observed for Ni/Ti sample (Fig. 1, *b*). However, the following annealing at 400°C leads to the emergence of a new set of diffraction peaks, in addition to the already existing Ni lines. The new peaks appear at 45.91°, 47.42°, and 56.37° diffraction angles that fit well to the (112), (211) and (013) peaks of orthorhombic NiSi silicide phase. This means that even a relatively low annealing temperature of 400°C is enough for the interdiffusion between Ni and Si resulting in the formation of the Ni monosilicide (the enthalpy of NiSi formation is −42,4 kJ/mole [17]). As worth to note, the formation of NiSi orthorhombic silicide is usually observed at higher annealing temperatures [18]. However, for the case of thin films, the activation energies are particularly lower compared to the bulk materials and the phase transitions are traditionally taking place at much lower temperatures than it could be expected from the corresponding binary diagrams. When the heat treatment temperature rises to 500°C, the NiSi silicide phase is further developed that is evidenced in the arising of new peaks (101), (002), (200), (102), (210), (103), (020) corresponding to the orthorhombic NiSi crystal structure. Simultaneously, the diffraction peaks from Ni vanish, indicating that the metal layer has been completely consumed in reaction with the Si substrate. Ultimately, there are no noticeable changes seen in the phase composition of the Ti/Ni sample when the temperature is further increased up to 600°C.

The values of Ni lattice constant (Fig. 2, *a*) are close for the as-deposited Ni/Ti and Ti/Ni films and are of ≈ 0.351 nm. Annealing at 400°C induces the slight drop of the Ni lattice constant to ≈ 0.350 nm for both thin-film systems, which is likely associated with the annealing of structural defects and relaxation of residual stresses formed at the deposition stage. For higher temperatures (> 400°C), only data for Ni/Ti bilayer are given due to the absence of Ni peaks on the XRD scans of Ti/Ni film caused by the appearance of silicides. It can be seen (Fig. 2, *a*) that annealing of Ni/Ti film at elevated temperatures of 500–600°C leads to the return of Ni lattice parameter to its initial value, which is most likely associated with the thermal expansion of Ni [19].

Figure 2, *b* shows the change of Ni crystallite size as a function of annealing temperature. The crystallite size (or coherence length) has been evaluated from the value of the full width at half maximum of Ni (200) diffraction pike using the Scherrer equation [20]. The typical grain recrystallization behaviour is observed during thermal annealing evidenced in the increase of the Ni crystallite size from 12–13 nm to 32–36 nm for both Ni/Ti and Ti/Ni samples. It should be noted that the increase of annealing temperature from 400°C to 500–600°C does not affect the average crystallite size that remains in the range of 30–

35 nm.

The change of initial layers configuration causes some difference of fundamental peak intensities of Ni phase. For instance, when Ni is deposited as a bottom layer, the ratio of $I(111)/I(200)$ is 3 times higher than when it is used as a top layer (Fig. 3, *c*). This discrepancy may be related to the presence of partial preferential grain orientation during the film growth; however, it is impossible to draw the clear conclusion now.

For a better understanding of the diffusion reactions, which take place in the studied thin-film systems upon heat treatment, the chemical depth profiling using dynamic SIMS technique was employed. SIMS spectra for thin Ni/Ti and Ti/Ni films after deposition and annealing in a vacuum at 500°C are shown in Fig. 3. The depth profile of Ni/Ti bilayer after deposition (Fig. 3, *a*) demonstrates a clear separation of Ni, Ti and Si layers. The different sputtering time of Ni and Ti layers

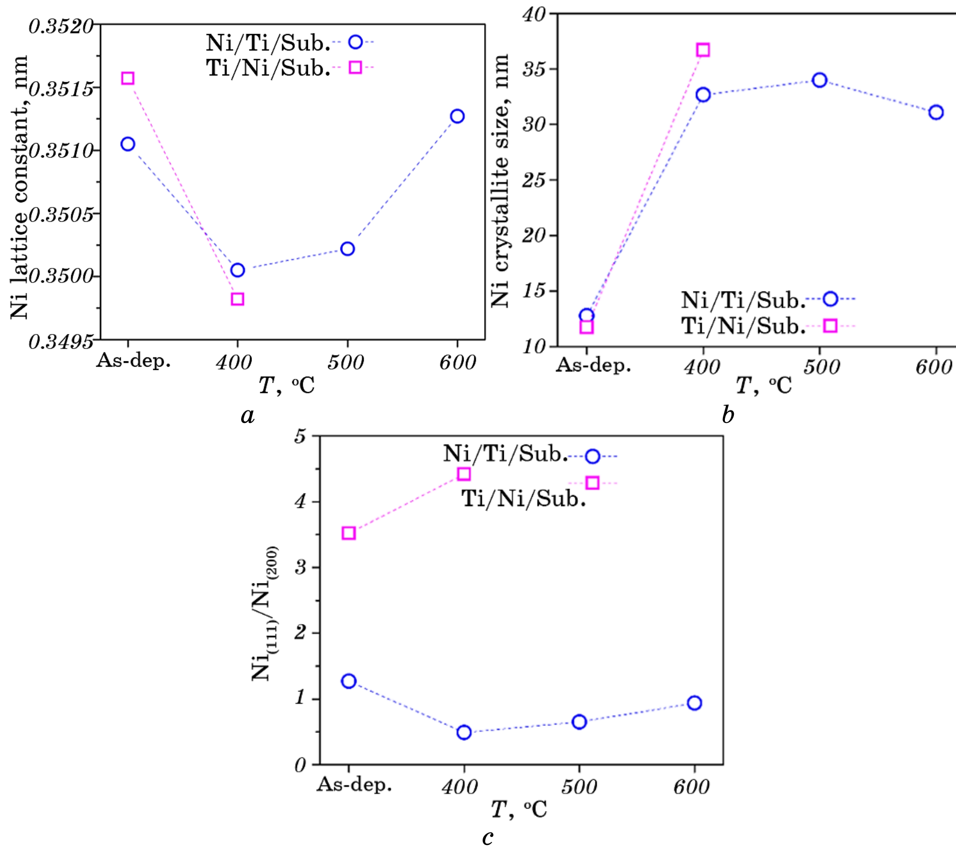

Fig. 2. The change of the nickel lattice constant and crystallite size of thin Ni/Ti films as a function of temperature.

observed at the depth profiles is attributed to the difference of their sputtering yields (1.9 nm/s and 0.8 nm/s for Ni and Ti, respectively).

Thermal annealing at a temperature of 500°C leads to the significant changes of in-depth elemental composition. For the case of Ni/Ti film (Fig. 3, *b*), the segregation of Ti atoms on the outer surface of the Ni layer is observed, which can be associated with the high affinity of Ti to oxygen. While there is no noticeable change of Ni signal distribution after annealing, a small splash of its intensity, which appeared at the surface, indicates the surface oxidation [21]. It can be concluded from the complex analysis of XRD and SIMS data that Ti atoms diffuse towards the outer surface *via* the Ni grain boundaries without interaction with Ni crystal lattice, since no intermetallic NiTi phases have been found at θ–2θ scans in detectable quantities.

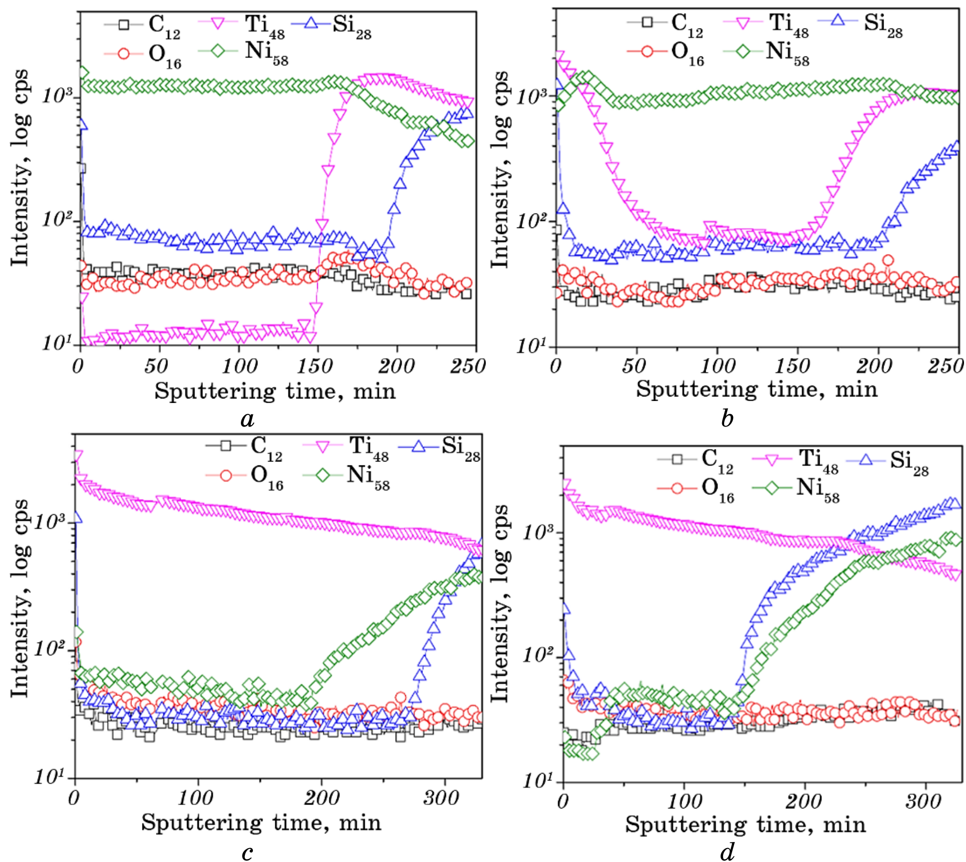

Fig. 3. SIMS elemental distribution of the as-deposited thin Ni/Ti (*a*) and Ti/Ni (*c*) films, as well as after annealing at 500°C for 1 hour (*b*, *d*, respectively).

For the case of Ti/Ni bilayer (Figure 3, *d*), the annealing at 500°C does not affect the initial depth distribution of Ti, whereas the interface between Ni layer and Si substrate completely vanishes and mutual intermixing of these layers is clearly observed. This observation is well agreed with the XRD data and affirms the NiSi silicide formation during annealing. Therefore, no visible marks of interdiffusion between Ti and Ni layers were observed in Ti/Ni stack, and the applied heat treatment in vacuum does not lead to the formation of NiTi intermetallics.

Ni–Ti thin-film system exhibits a large negative Gibbs energy of mixing, which contributes to the interfacial solid-state reactions and amorphization taking place even under local heating conditions [22]. However, the Ni–Ti amorphization could lead to a rise of Gibbs free energy and slowdown of the diffusion processes [23]. In the present case, the Ti layer has been formed in the amorphous state right after deposition and remained amorphous even after annealing at elevated temperatures, so that can affect the Ni reaction with silicon substrate instead of Ni–Ti interdiffusion. From the thermodynamic point of view, the formation of NiSi monosilicide is more preferable since it has lower enthalpy of formation (ranging from −42.4 kJ/mole to −67.3 kJ/mole [17]) as compared to the Ni_xTi_y intermetallic phases (−25.3 ± 1.7 kJ/mole for $NiTi_2$, −31.1 ± 1.1 kJ/mole for NiTi and −43.8 ± 1.6 kJ/mole for Ni_3Ti, respectively [24]).

4. CONCLUSIONS

This study is aimed to explore the effect of Ni and Ti layers arrangement on the diffusion and phase formation in submicron Ni/Ti and Ti/Ni films magnetron sputtered on Si (100) single-crystal substrate and next annealed up to 600°C in a vacuum. XRD data revealed the formation of polycrystalline Ni phase and amorphous Ti in both systems after deposition. However, the significant discrepancy between studied bilayers has been observed in the diffusion behaviour of its components upon heat treatment. When Ni is applied as a top layer, the vacuum annealing leads to the overwhelming Ti atomic diffusion towards the outer surface through the Ni grain boundaries and its agglomeration at the surface. This process is likely induced by the high affinity of Ti to oxygen. On the other hand, in the case of annealing of a film with Ti top layer, no interdiffusion between Ni and Ti layers is taking place, while Ni completely consumes in reaction with Si substrate. Therefore, the diffusion-induced phase formation in Ni–Ti bilayers strongly depends on the spatial layers arrangement which should be taken into account and adjusted depending on the application goals.

This work was supported by the Grant (No. 0121U110283) from the

Ministry of Education and Science of Ukraine.

REFERENCES

1. J. Sevcikova and M. Pavkova Goldbergova, *Biometals*, **30**, No. 2: 163 (2017).
2. M. Mehrpouya and H. Cheraghi Bidsorkhi, *Micro Nanosystems*, **8**, No. 2: 79 (2016).
3. A. Behera and S. Aich, *Surf. Interface Analysis*, **47**, No. 8: 805 (2015).
4. E. Horache, J. Van Der Spiegel, and J. E. Fischer, *Thin Solid Films*, **177**, Nos. 1–2: 263 (1989).
5. S. P. Murarka, *Intermetallics*, **3**, No. 3: 173 (1995).
6. N. Sharma, K. K. Jangra, and T. Raj, *Proc. Institution of Mechanical Eng., Part L: J. Materials: Design Applications*, **232**, No. 3: 250 (2018).
7. H. Cho, H. Y. Kim, and S. Miyazaki, *Sci. Technol. Adv. Mater.*, **6**, No. 6: 678 (2005).
8. T. Lehnert, H. Grimmer, P. Böni, M. Horisberger, and R. Gotthardt, *Acta Mater.*, **48**, No. 16: 4065 (2000).
9. T. Lehnert, S. Tixier, P. Böni, and R. Gotthardt, *Mater. Sci. Eng. A*, **273**: 713 (1999).
10. H. Aboulfadl, F. Seifried, M. Stueber, and F. Muecklich, *Mater. Lett.*, **236**: 92 (2019).
11. T. Krist, M. Briere, and L. Cser, *Thin Solid Films*, **228**, Nos. 1–2: 141 (1993).
12. A. Behera, S. Aich, A. Behera, and A. Sahu, *Mater. Today: Proc.*, **2**, Nos. 4–5: 1183 (2015).
13. A. Behera and S. Aich, *Surf. Interface Analysis*, **47**, No. 8: 805 (2015).
14. L. Neelakantan, S. Swaminathan, M. Spiegel, G. Eggeler, and A. W. Hassel, *Corrosion Sci.*, **51**, No. 3: 635 (2009).
15. P. Scherrer, *Bestimmung der Inneren Struktur und der Größe von Kolloidteilchen mittels Röntgenstrahlen* [Determination of the Internal Structure and Size of Colloidal Particles Using X-Rays] (Berlin: Springer: 1912), p. 387 (in German).
16. H. J. Lee and A. G. Ramirez, *Appl. Phys. Lett.*, **85**, No. 7: 1146 (2004).
17. M. E. Schlesinger, *Chem. Rev.*, **113**, No. 10: 8066 (2013).
18. F. Deng, R. A. Johnson, P. M. Asbeck, S. S. Lau, W. B. Dubbelday, T. Hsiao, and J. Woo, *J. Appl. Phys.*, **81**, No. 12: 8047 (1997).
19. A. J. Saldivar-Garcia and H. F. Lopez, *Metallurgical Mater. Trans. A*, **35**, No. 8: 2517 (2004).
20. Zoleikha Hajizadeh, Reza Taheri-Ledari, and Fereshteh Rasouli Asl, *Heterogeneous Micro and Nanoscale Composites for the Catalysis of Organic Reactions* (Ed. A. Maleki) (Elsevier: 2022), p. 33.
21. S. Perusin, D. Monceau, and E. Andrieu, *J. Electrochem. Society*, **152**, No. 12: E390 (2005).
22. A. J. Cavaleiro, R. J. Santos, A. S. Ramos, and M. T. Vieira, *Intermetallics*, **51**: 11 (2014).
23. T. Mousavi, M. H. Abbasi, and F. Karimzadeh, *Mater. Lett.*, **63**, Nos. 9–10: 786 (2009).
24. Z. Moser, W. Gąsior, K. Rzyman, and A. Dębski, *Archives of Metallurgy and Materials*, **51**, No. 4: 606 (2006).